



Review Article: Applications and Methods of Preparation of Iron Oxide Fe_3O_4 Nanoparticle

By Marwa Yousef Freshik & Fathi Mohammed Asseid

Zawia University

Abstract- Metal Oxide Nanoparticles are of interest in modern research and applications. Fe_3O_4 nanoparticles have interesting properties that can be manipulated in a various applications, some of these applications represent an advanced technology to biological and medical sciences [1-5], drugs and gene mapping [6-9], Detection of proteins moieties [10], Tumour removal [11,12] bioanalysis of pathogens [13], Tissue analysis [14], monitoring of DNA structure [15,16], and Magnetic Resonance Imaging resolution improvement [18-23] chromatographic separation and purification of molecules and biological cells [24]. The purpose of this review is to summarize the different methods of preparations of Fe_3O_4 nano particles and describes these methods of preparation allowing control of the size, morphology, and surface treatment. These nanoparticles can be prepared by different methods such as Gas, liquid, two-phase methods, Sol-gel methods, High pressure hydrothermal methods and Co-precipitation Method.

GJSFR-B Classification: FOR Code: 259999



Strictly as per the compliance and regulations of:



Review Article: Applications and Methods of Preparation of Iron Oxide Fe₃O₄ Nanoparticle

Marwa Yousef Freshik ^α & Fathi Mohammed Asseid ^σ

Abstract- Metal Oxide Nanoparticles are of interest in modern research and applications. Fe₃O₄ nanoparticles have interesting properties that can be manipulated in a various applications, some of these applications represent an advanced technology to biological and medical sciences [1-5], drugs and gene mapping [6-9], Detection of proteins moieties [10], Tumour removal [11,12] bioanalysis of pathogens [13], Tissue analysis [14], monitoring of DNA structure [15,16], and Magnetic Resonance Imaging resolution improvement [18-23] chromatographic separation and purification of molecules and biological cells [24]. The purpose of this review is to summarize the different methods of preparations of Fe₃O₄ nano particles and describes these methods of preparation allowing control of the size, morphology, and surface treatment. These nanoparticles can be prepared by different methods such as Gas, liquid, two-phase methods, Sol-gel methods, High pressure hydrothermal methods and Co-precipitation Method.

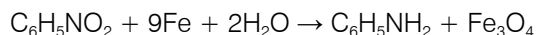
1. INTRODUCTION

Iron(III)oxide Fe₃O₄ a ferromagnetic metal oxide is one of several iron oxides and a member of the spinel structural group (of inverse type) [25,26]. The systematic name is iron (II, III) oxide. Also known as magnetite mineral whose chemical formula can be written as FeO•Fe₂O₃, a composition of wustite (FeO) and hematite (Fe₂O₃). This formula reflects the different oxidation states of the iron in the spinel inverse type structure.

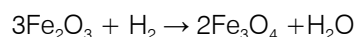
The dimensions of iron oxide nanoparticles are generally described by its diameters that are between 1 and 1000 nanometers. The forms magnetite (Fe₃O₄) and its oxidized form Maghemite (Fe₂O₃) are synthesized, well characterized, and attracted a number of research groups due to their magnetic properties and potential for use in many technical applied sciences. These mineral do not pose any toxicity threats and environment friendly type of oxides with respect to other transition metal oxides, which are highly magnetic materials, known to be toxic and easily oxidized.

Row quality Fe₃O₄, usually called synthetic magnetite, can be prepared using by processing industrial wastes, and scrap iron or solutions containing iron salts (by-products of industrial processes such as the acid treatment of steel, through the following steps:

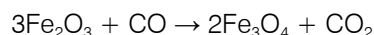
1. Oxidation of Fe metal by the Lucas process. Treatment of nitrobenzene with iron metal in presence of iron chloride, FeCl₂ as a catalyst to form in Fe₃O₄



2. Oxidation of Fe²⁺ compounds, to precipitate iron(II) salts as hydroxides followed by oxidation by aeration and the oxide produced determined by careful control of the pH.
3. Reduction of Fe₂O₃ with hydrogen [28]:



4. Reduction of Fe₂O₃ with CO:



Production of nano-particles can be done chemically by mixing salts of Fe^{II} and Fe^{III} and followed by addition of alkali to precipitate Fe₃O₄ in colloidal form. Control of the conditions of the reaction are important to the determination of the particle size desired.

Magnetite exhibits a cubic inverse spinel structure in which oxygen forming a face centered cubic closed packing structure (Fig 2.6). With, the tetrahedral sites are occupied by Fe³⁺ and octahedral sites are occupied by both Fe³⁺ and Fe²⁺ ions. Maghemite and Magnetite minerals are different structurally from each other. In Magnetite mineral most of the iron ions are trivalent (Fe³⁺) accompanied by the presence of cationic vacancies within the octahedral sites. Maghemite mineral exhibits a cubic unit cell, each cell contains 32 O ions, 21 1/3 Fe³⁺ ions and 2 1/3 vacancies. The iron ions are distributed randomly over the 8 tetrahedral and 16 octahedral sites.

Author ^α: Physics department, Zawia University.

Author ^σ: Chemistry department, Zawia University.

e-mail: asseidfathi6@gmail.com

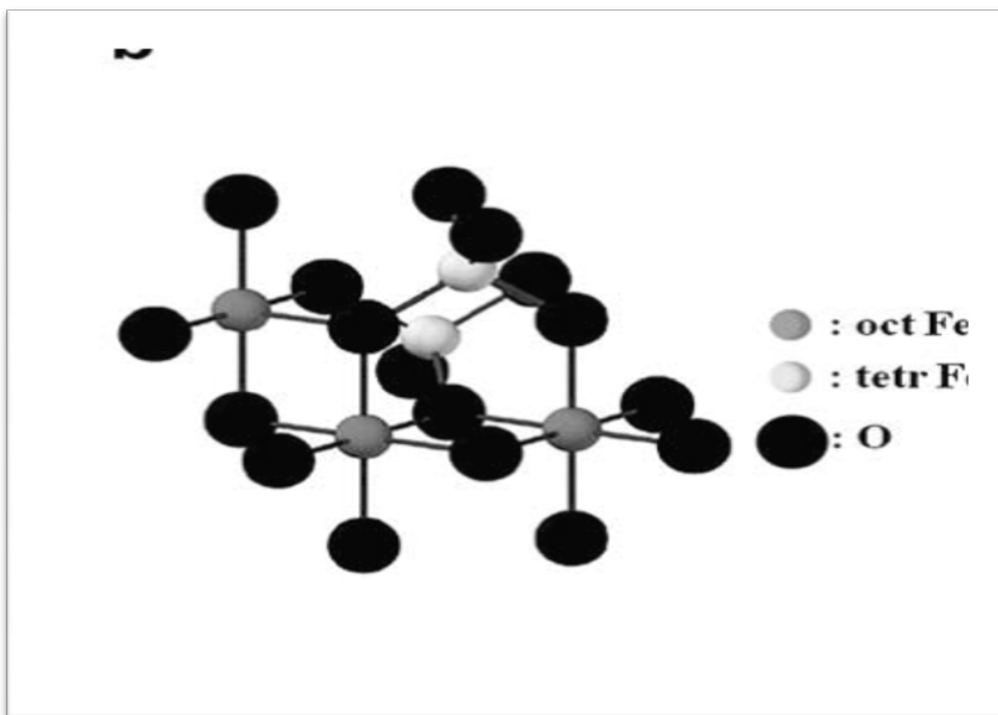


Fig. 2.6: Crystal structures of magnetite, Adapted from ref [27]

Fe₃O₄ is ferromagnetic with a phase transition at 120K, the so-called Verwey transition, in which there is a discontinuity in the structure, conductivity and magnetic properties. This effect has been extensively investigated with a number of explanations were proposed, however it is not fully clear. Fe₃O₄ exhibits electrical conducting

property with conductivity significantly higher (x 10⁶) than that of Fe₂O₃, this is due to electron exchange between the Fe^{II} and Fe^{III} centers. Physical and magnetic properties for Magnetite are summarized in Table 2.3.

Table 2.3: Physical and magnetic properties of iron oxides

Property	Oxide (Magnetite)
Molecular formula	Fe ₃ O ₄
Density(g/cm ³)	5.18
Melting point (°C)	1583
Hardness	5.5
Type of magnetism	Ferromagnetic
Curie temperature (K)	850
MS at 300 K (A-m ² /kg)	92-100
Standard free	-1012.6
Crystallographic	Cubic
Structural type	Inverse spinel
Space group	Fd3m
Lattice parameter(nm)	a=0.8396

It is well known fact that iron atom has a strong magnetic moment as a result of four unpaired electrons in its 3d orbitals. Formation of crystals of iron atoms due to different magnetic states as shown in Fig. 2.7. The paramagnetic state, usually arise paired electrons in its 3d orbitals of the individual atomic magnetic moments randomly aligned with respect to each other, so the crystal has a zero net magnetic moment. However, if this crystal is exposed to an external magnetic field, some of these moments align,

and the crystal will attain a small net magnetic moment. In the case of ferromagnetic crystal, all the individual moments are aligned without an external field effect. The ferromagnetic crystal, however has a net magnetic moment result from two types of atoms with moments of different magnetic strengths arranged anti parallelly (Fig. 2.7). When anti parallel magnetic moments are similar in magnitude, the crystal is known as anti ferromagnetic and possesses net magnetic moment of zero.

Bulky ferromagnetic material, in which the magnetization M is the vector sum of all the magnetic moments of all the atoms per unit volume of the material. The magnitude of M is generally less than its value when all atomic moments are totally aligned, because the bulk material consists of domains, with each domain is having its own magnetization vector resulting from the alignment of atomic magnetic

moments within the domain (Fig. 2.8). The magnetization vectors of all the domains in the material may not be aligned, and this leads to a decrease in the overall magnetization (Fig. 2.8). During the length scale of the material becomes small, the number of domains decrease until there is a single domain at which the characteristic size of the material is below some critical size d_c [27].

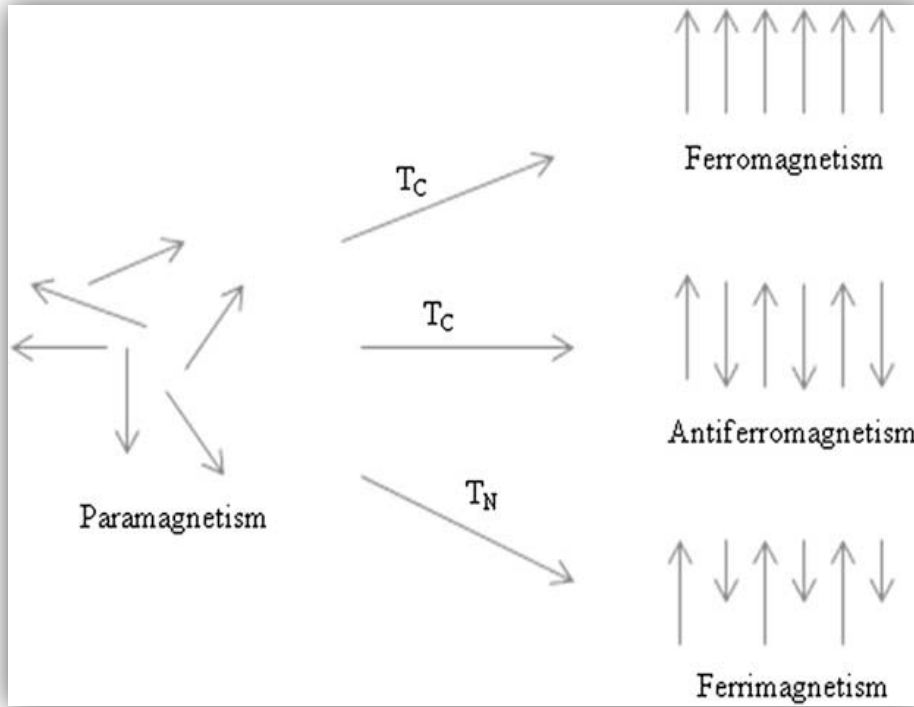


Fig. 2.7: Alignment of individual atomic magnetic moments in different types of materials. Adapted from ref [27]

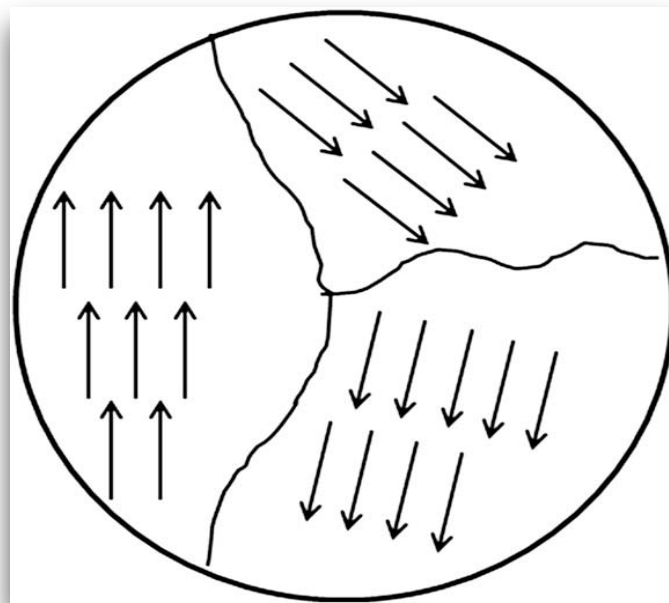


Fig. 2.8: Magnetic domains in a bulk material

Whenever an external applied magnetic field of H is introduced to a ferromagnetic materials of magnetic strength M , the magnetization curve obtained, Fig. 2.9 showing that M increases with H until a saturation value M_s is reached. The magnetization curve displays a hysteresis loop, because all domains do not stabilize to the original state of orientations when H is decreased after the saturation magnetization value is attained. Consequently, when H returns back to zero, there is a

remnant magnetization M_R which can only be removed by having a coercive field H_C applied in the opposite direction to the initially applied field. A single domain magnetic material does not show similar loop and is said to be super paramagnetic. Iron oxide nanoparticles of size smaller than about 20 nm often display super paramagnetic behavior at room temperature a character usually demanded in nanoparticle materials.

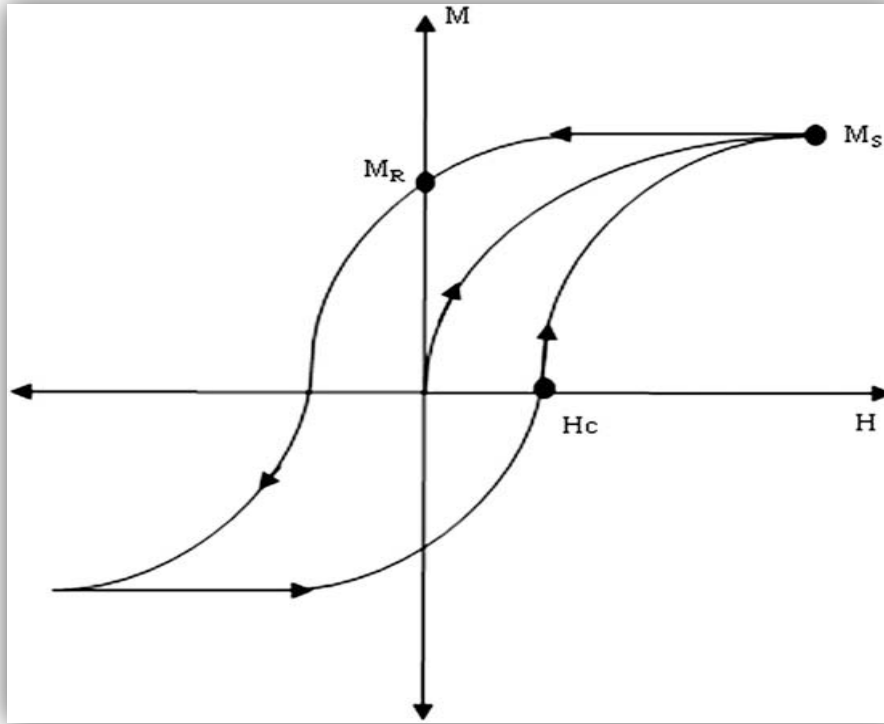


Fig. 2.9: Magnetization M as a function of an applied magnetic field H

Ordered arrangement of magnetic moments decrease with increasing temperature due to thermal fluctuations of the individual moments. Beyond the Neel or Curie temperature, the material in this case becomes disoriented and loses its net magnetization. The transition temperature is known as the Curie temperature T_C for ferromagnetic substances, and the Neel temperature T_N for anti ferromagnetic substances. Super paramagnetic particles are usually ordered below a blocking temperature, T_B . Magnetite is ferrimagnetic at room temperature and has a Curie temperature of 850 K. Magnetite particles smaller in size than 6 nm are super paramagnetic at room temperature, although their magnetic properties depend strongly on the methods of preparation used in their synthesis.

Tartaj and co-workers., reported that the magnetic properties of Nano sized magnetite depending strongly on changes in the crystal morphology[29]. The crystal morphology has coercivity factor in the order of: spheres < cubes < octahedra with increasing the number of magnetic axes along this series of shapes.

Magnetite particles with coercivities ranging from 2.4 to 20 kA/m have been produced by controlling their synthetic conditions.

Surface effects influence the magnetic properties of iron oxide nanoparticles. As a result, iron oxide nanoparticles net magnetization decreases at a fast rate with increasing temperature higher than that of the corresponding bulk material because a large number of the atoms near the surface where the exchange field is low. Modifications of the surface by chemical treatments enhances the coercivity of oxide nanoparticles. This is due to the dependence on size and surface treatment, and nano structuring of magnetic materials through the method of preparation can be used to improve magnetic properties, this will be discussed below.

II. APPLICATIONS OF Fe_3O_4

The magnetic properties of iron oxides have been used in a wide range of applications including, catalysts, magnetic seals and inks, magnetic recording

media, and ferro-fluids, in addition to contrast agents for magnetic resonance imaging (MRI) and therapeutic agents for cancer treatment. These applications require nanomaterials of specific sizes, shapes, surface characteristics, and magnetic properties.

Usage in data storage applications, the particles must have a stable, switchable magnetic state that is unaffected by temperature variations. For high performance in recording, the particles should exhibit both high coercivity and high remanence, and they should be uniformly small, and resistant to corrosion, friction, and temperature changes [27].

Magnetite used in ferro-fluids was proposed to optimize performance seals in space technology applications. Ferro-fluids is composed super paramagnetic nanoparticles dispersed in aqueous or organic solvents. This type of fluid has net magnetic moment when subjected applied field. An external field is therefore able to trap the fluid in a specific location to become a seal. Ferro-fluids exhibits properties such as magnetic field dependent optical anisotropy proved to be useful in optical switches, and tunable diffraction gratings. They are usually used in sealing computer disk units, and in vibrating environments in place of regular seals. Ferro-fluids are also use in NMR probes for receiving and transmitting coils, they have also been suggested for use in eye surgery to repair damaged retinas. Ferro-fluids are shown to have a high degree of colloidal stability in a magnetic field gradient. One of the keys to improving their performance in these applications is to make the particles smaller and more uniform, which requires an optimum method of preparation.

The application of magnetite nanoparticles received significant interest in last decade specially in magnetic resonance imaging contrast agents, and targeted drug delivery vehicles, as well as in magnetic hyperthermia. These applications demand particles that exhibit super paramagnetic property at room temperature. Magnetization is controlled to desired levels as excess magnetization sometimes lead to agglomeration of these nanoparticles, and this could lead to blockage of blood vessels. In addition, applications in biology and medical diagnosis require stable magnetic nanoparticles in water at neutral pH and physiological conditions. The colloidal stability of magnetic fluids depends on the size of particles, which should be sufficiently small to minimize precipitation due to gravitation forces, and on the charge and surface chemistry. Magnetite is the most commonly employed materials for biomedical applications[30].

Focused attention on the use of Magnetite in biomedical applications due to their biocompatibility and lower toxic effect in the human body. A major area of applications has been in the field of bio-assays where the magnetic properties have been exploited in vitro to manipulate magnetite nanoparticles with an external

magnetic field. Wang andco-workers have developed extremely sensitive magnetic microarrays using ferromagnetic sensors to detect binding of target DNA and proteins [31].

Magnetic nanoparticles have been used in vivo as magnetic resonance imaging (MRI)contrast agents for molecular and cell imaging. Super paramagnetic magnetite is used as the core in these agents which are used to differentiate between healthy and unhealthy tissues and cells. The superparamagnetic nanoparticles are coated with a polysaccharidic layer for colloidal stability and better sensitivity. In vivo MRI cell tracking has been successfully performed by Song and co-workers[32]. Magnetic nanoparticles with a polymer coating have been used in cell separation, protein purification, environment and food analyses, organic and biochemical syntheses, industrial water treatment and biosciences. Encapsulation of magnetic nanoparticles with organic polymers is used to enhance their chemical stability, dispersability and functionality [33].

Another important application of magnetic nanoparticles is hyperthermia in cancer therapy. Super-paramagnetic magnetic nanoparticles when exposed to an alternating magnetic field can be used to heat tumor cells to 41-45°C, where tissue damage of normal tissue is reversible while the tumor cells are irreversibly damaged, a process constitutes a giant step in irradiating cancerous cells.

Magnetite is used industrially as catalysts for a number important reactions, including the synthesis of NH_3 (the Haber process), the high temperature water gas shift reaction, and the desulfurization of natural gas[34]. Other reactions include the dehydrogenation of ethyl benzene to styrene, the Fisher-Tropsch synthesis for hydrocarbons, the oxidation of alcohols, and the large scale manufacture of butadiene.

Magnetite is semiconductors and can catalyze oxidation/reduction reactions. Iron oxides can be used as acid/base catalysts and to catalyze the degradation of acrylnitrile-butadiene-styrene copolymer into fuel oil.

Magnetic iron oxide is commonly used in synthetic pigments in paints, ceramics, and porcelain. Pigments made from magnetite are also used in magnetic ink character recognition devices, and super paramagnetic magnetite particles are used in metallography for detecting flaws in engines[35].

As noted above, many of the useful attributes of iron oxides depend on the preparation method for the nanomaterials. The preparation method plays a key role in determining the particle size and shape, size distribution, surface chemistry and therefore the applications of the material. In addition, the preparation method also determines the degree of structural defects or impurities present in the particles, and the distribution of such defects. Many synthetic routes have been developed to achieve proper control of particle size,

polydispersity, shape, crystallinity, and the magnetic properties. Some of these methods are described in the following sections.

III. METHODS OF PREPARATION

a) Gas phase method of preparation of metal oxide nanoparticles

These methods of preparations of nanomaterials depend on thermal decomposition (pyrolysis), reduction, hydrolysis, disproportionation reactions, oxidation/reduction, and other reactions to precipitate solid nano materials from the gas phase form. Chemical Vapor Deposition (CVD) process, allows for a carrier gas stream with precursors to be delivered continuously by a gas delivery system to a reaction chamber under vacuum at high temperature, above 900°C. This type of reaction takes place in the heated reaction chamber and the precursors combine to form nanoparticles. Growth and agglomeration of the nanoparticles are mitigated through rapid expansion of the two-phase gas stream at the outlet of the reaction chamber (Fig.2.10). A follow-up heat treatment of the synthesized nano powders in various high-purity gas streams allows for compositional and structural modifications, including nanoparticle crystallization, and transformation to a desirable size, composition, and morphology [36]. This process employed to deposit iron

oxide through the reaction of iron halide, such as iron trichloride, with water, heated to 800-1000°C. The success of this method depends on control of concentrations of precursor in the carrier gas, as well as rapid expansion and quenching of the nucleated clusters or nanoparticles as they exit from the reactor [37]. The use of organometallics as precursors in the MOCVD process, allows reactions to take place at lower temperature range 300-800°C and at pressure varying from less than 1torr to ambient conditions. Iron oxide thin films have been produced via reaction of thermal decomposition of acetylacetonate at 400-500°C, and iron trifluoro-acetylacetonate at 300°C in oxygen (Singh et al .2008) [38a]. Precursors include tris(2,2,6,6-tetramethyl-3,5-heptadionato) Fe(III) and tris-t-butyl-3-oxo-butanoato Fe(III) were also used. Recently, Park et al. [38b] deposited magnetite thin films using Fe(II) dihydride complexes $H_2Fe[P(CH_3)_3]_4$ at 300°C in oxygen by direct growth of magnetite has been achieved by a low-pressure CVD using metal-organic ferric dipivaloyl-methanate as a precursor. Upon oxidation, these films were converted to maghemite. Another MOCVD reaction uses microwave plasma to decompose either iron cyclopentadienyl in an oxygen atmosphere at 300-500°C and 1-20 Tor pressure.

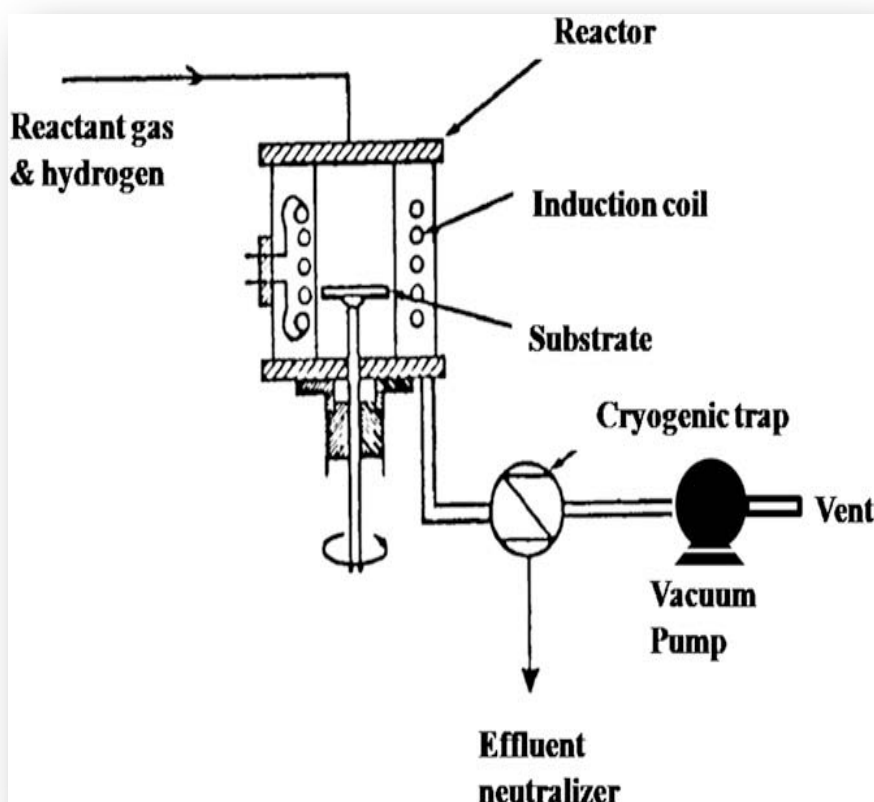


Fig. 2.10: Schematic diagram of a CVD apparatus (Adapted from ref [39]).

Laser pyrolysis of organometallic precursors based on resonant interaction between laser photons and gaseous species, reactant or sensitizer. Either of these energy transfer agents that is excited by absorption of CO_2 laser radiation and transfers the absorbed energy to the reactants by collision [40]. The method involves heating a flowing mixture of gases with a continuous wave CO_2 laser to initiate and sustain a chemical reaction until a desired concentration of nuclei is reached in the reaction, which leads to homogeneous nucleation of particles. A schematic representation of a CO_2 laser pyrolysis device is shown in Fig.2.11. The nucleated particles formed during the reaction are driven by the gas stream and collected at the exit [29].

Well-crystallized and uniform iron oxide nanoparticles, including nanoparticles of hematite and maghemite, were obtained through one step using laser pyrolysis. Iron pentacarbonyl is usually used as a precursor in this method and ethylene is used as the

carrier gas to transport the carbonyl vapor to the reaction chamber, this is because ethylene does not absorb radiation at the laser wavelength. The iron pentacarbonyl breaks to iron and carbon monoxide molecules, followed by oxidation using air, then introduced into the system with the iron pentacarbonyl vapor or mixed with argon. Iron particles with 14 nm mean diameter and about 4 nm oxide shell thickness have been produced by this procedure of iron pentacarbonyl and ethylene mixtures followed by a controlled step-by-step passivation process [41].

The effect of process conditions on the structural and magnetic properties of maghemite nanoparticles produced by laser pyrolysis have been studied by Verdaguer et al.(2002) [42]. They reported that the particle size depends on the oxygen content of the gas phase and is independent of the laser conditions, and suggested that the amount of oxygen be used to optimize the size and crystallinity of the particles.

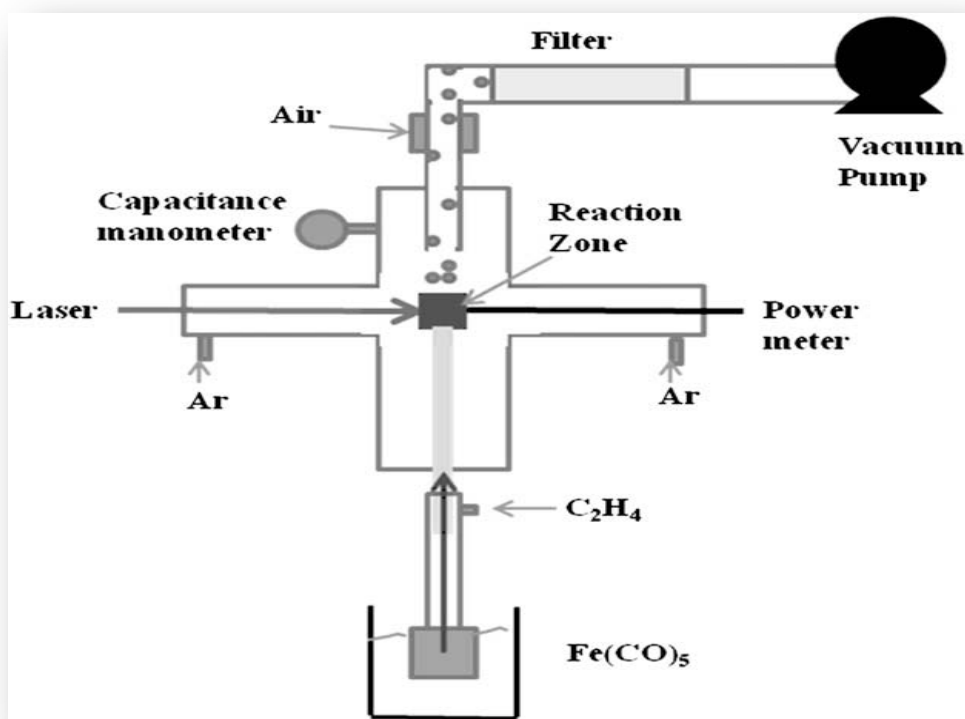


Fig. 2.11: Schematic diagram of a CVD apparatus (Adapted from ref[29])

Although gas phase methods are able to deliver high quality products, the yields are usually low and scale-up can be maintained. Variables such as oxygen concentration, gas phase impurities, and the heating time must be controlled precisely to obtain pure products.

b) Liquid phase methods of preparation of metal oxide nanoparticles

Liquid phase methods are more practical, generally affordable, and offer better yields of products

as well as ease of surface modifications. Most nanoparticles prepared by such methods have been via coprecipitation from aqueous solutions, although other organic solvents can also be used. It has been shown that magnetite particles with mean diameters ranging from 30 to 100 nm can be achieved by the reaction of a Fe (II) salt, a base and a mild oxidant (nitrate ions) in aqueous solutions. Stoichiometric amounts of ferrous and ferric hydroxides can also be reacted in aqueous media to yield homogeneous spherical particles of either magnetite or maghemite. The phase and size of

the particles depend on contents of cations, the counter ions present, and the pH of the solution. However, it is possible to control the mean size of the particles by adjusting the pH and the ionic content.

Due to the large surface-area to volume ratio, nanoparticles formed by liquid phase coprecipitation tend to aggregate in solution in order to reduce their surface energy. The suspension of nanoparticles can be stabilized by adding anionic surfactants as dispersing agents. The nature of the counterions, pH, and ionic strength can then be used to stabilize the charged particles via interactions between electrical double layers. Increasing the concentration of inert electrolyte in the system compresses the double layer and promotes coagulation. However, suspensions of iron oxide that are stabilized entirely by electrostatic repulsion are too sensitive to external conditions such as pH and ionic strength to offer any flexibility in engineering the surface properties of the particles.

Stabilization can also be achieved by coating the particle surfaces with proteins, starches, non-ionic detergents, or polyelectrolytes. Adsorption of such substances stabilizes the particles at electrolyte concentrations that would otherwise be high enough for coagulation to occur. Charles [43] prepared water-based magnetic fluids by dispersing magnetite particles in water containing oleic acid. Khalafalla & Reimers (1980) [44] also produced stable aqueous magnetic fluids using dodecanoic acid as a dispersing agent. Usage of saturated and unsaturated fatty acids to stabilize magnetic fluids has been intensively studied.

Better quality monodisperse and monocrystalline iron oxide nanoparticles can be produced by the thermal decomposition of organo metallic precursors in organic solvents containing stabilizing surfactants such as oleylamine, oleic acid, and steric acid. Precursors that have been investigated include iron acetylacetonate, iron carboxylate, iron cupferronates and iron carbonyls. High quality magnetite nanoparticles with diameters ranging from 3 to 20 nm were synthesized via thermal decomposition of Fe(III) acetylacetonate in phenyl/benzyl ether and 2-pyrrolidone.

Recently, Novak et al.[45] investigated the synthesis of maghemite by thermal decomposition of some complex combinations of Fe(III) with carboxylate type ligands obtained from the redox reaction between polyols and ferric nitrate. Maghemite was obtained at 250-300°C and hematite at 400-500°C.

Sun and co-workers [64a] have reported the preparation of mono disperse iron oxide nanoparticles by the thermal decomposition of iron acetylacetonate. They also proposed a simple method to transform hydrophobic nanoparticles into hydrophilic ones by adding bipolar surfactants and produced 4 nm magnetite nanoparticles by decomposition of Fe(III)

acetylacetonate in a mixture of phenyl ether, 1,2-hexadecanediol, oleic acid, and oleylamine . It has also been reported that 6-7 nm maghemite nanoparticles can be produced via the reaction of iron cupferronates with trioctylamine at 300°C. Maghemite nanoparticles with sizes ranging from 4 to 16 nm have been produced by decomposition of iron pentacarbonyl in octylether and oleic acid or lauric acid. These results show the effectiveness of the thermal decomposition method for the synthesis of iron oxide nanoparticles. However, the presence of residual surfactants may hamper the efficiency of subsequent surface modification of the synthesized nanoparticles. In addition, the use of toxic solvents and surfactants may be detrimental to the biocompatibility of the product [46b].

c) *Two-phase methods of preparation of metal oxide nanoparticles*

Water-in-oil microemulsions consisting of nanosized water droplets dispersed in an oil phase and stabilized by surfactant molecules at the water/oil interface usually used to obtain iron oxide nanoparticles. The surfactant-covered water pools show a unique microenvironment for the production of nanoparticles and limiting their growth. The size of the microemulsion droplets is determined by the water to surfactant ratio, although the overall size of the nanoparticles may also be influenced by factors such as concentration of reactants, and flexibility of the surfactant film [47].

Pialli and co-workers [48] studied a number of ways to manipulate microemulsions to synthesize nanoparticles. They reacted A and B by dissolving in the aqueous phases of two identical water-in-oil microemulsions and formed AB precipitate upon mixing (see Fig. 2.12a). The precipitate from droplets, hence limiting the size and shape of the particle formed as targeted. Alternatively, nanoparticles are produced by the addition of a reducing agent to a microemulsion containing the primary reactant in the aqueous phase (Fig. 2.12b). Fig. 8c outlines the formation of oxide, hydroxide or carbonate products by passing gases like O_2 , NH_3 , or CO_2 through a microemulsion containing salts of the cations [48].

Water-in-oil microemulsions have been also used to produce iron oxide, metallic iron nanoparticles, magnetic polymeric iron oxide nanoparticles, and silica-coated iron oxide nanoparticles. Various surfactants have been used when preparing these materials, including bis(2-ethylhexyl) sulfosuccinate, sodium-dodecyl sulfate, cetyltrimethylammonium bromide, polyvinylpyrrolidone, diethyl sulfosuccinate[49].

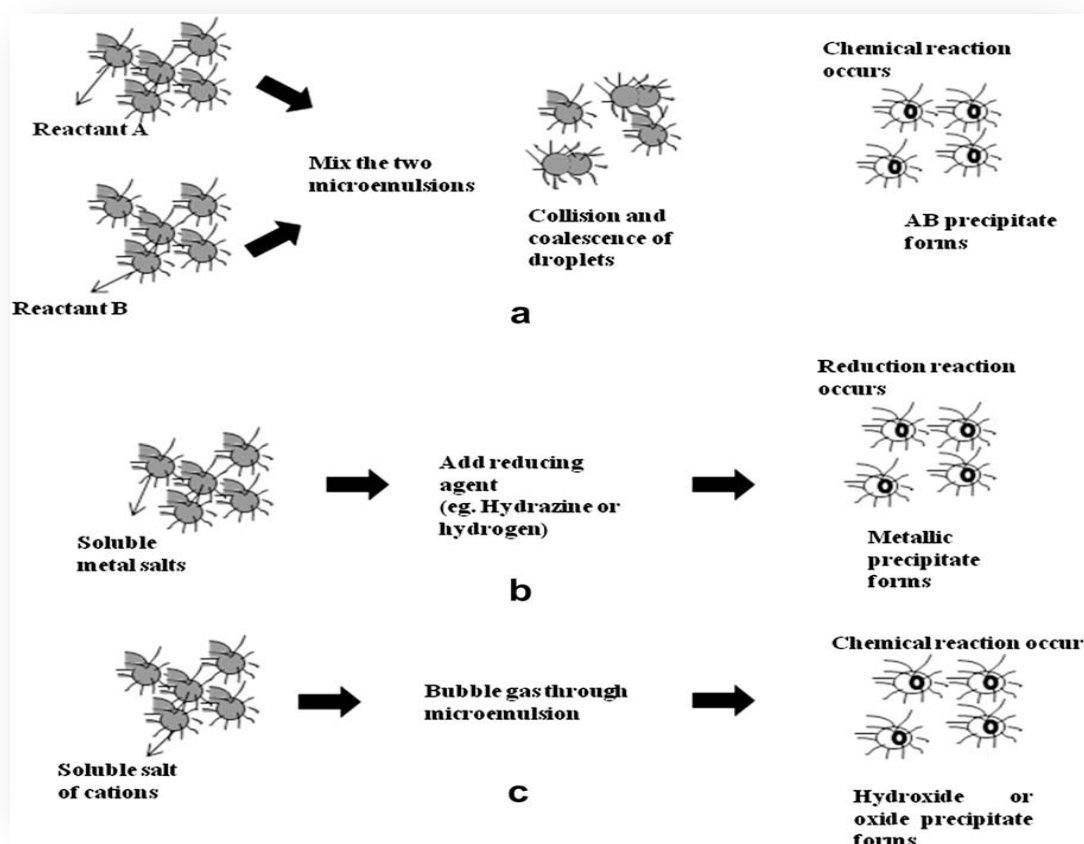


Fig. 2.12: Nanoparticle synthesis in microemulsions (a) by mixing two microemulsions, (b) using a reducing agent, and (c) by passing gas through the microemulsion [48]

d) Sol-gel method of preparation of metal oxide nanoparticles

Sol-gel methods, well developed methods for preparation of metal oxides nanoparticles, it refer to the hydrolysis and condensation of metal alkoxides or alkoxide precursors, resulting in dispersions of oxide particles in a sol. The sol is then dried or gelled by means of solvent removal or by chemical hydrolysis. The precursors can also be hydrolyzed by an acid or base media. Basic catalysis leads to the formation of a colloidal gel, whereas acid catalysis produces a polymeric gel. The rates of hydrolysis and condensation are the parameters that control the properties of the end products. Usually smaller particle sizes are obtained at lower controlled hydrolysis rates. The particle size also depends on the solution mixtures, pH value, and temperature. Magnetism of the sol-gel system relies on the resulting phases formed and the particle volume fraction, and is sensitive to the size distribution and dispersion of the nanoparticles. Nanocomposites extracted from gels, structural parameters and material porosity are determined by how fast the hydrolysis and condensation gel precursors, and by other oxidation-reduction side reactions that occur during the gelling and subsequent heat treatment [36].

Iron oxidesilica aerogels have been prepared by the sol-gel methods mentioned above, and found to be more reactive than conventional iron oxide. The increase in reactivity most likely due to the large surface area of iron oxide nanoparticles supported on the silica Aerogel. Precursors, TEOS and Fe(III) solutions are dissolved in an alcoholic aqueous media, and the gels produced after a few days calcined to produce the final desired materials. Ferric nitrate, ferric acetylacetonate and ferricchloride are the candidate metal oxide precursors, even though the use of the metallic complex FeNa(EDTA) and a mixture of this metallic complex with ferric nitrate has also been reported. Experimental work with pure metallic complex resulted in iron oxide nanoparticles in the size range 20-160 nm. Low solubility of EDTA salt in the solvent prevented the synthesis of high iron content aerogels when this complex is used as a precursor [50]. Aerogels generated from both pure ferric nitrate and its mixture with the metallic complex show low saturation magnetization values of 14 and 8.5 emu/g, respectively. This compares with bulk maghemite values of 74-76 emu/g. The low magnetization values suggest that the aerogels may not be suitable for magnetic applications, although they may still be useful in catalysis and other applications.

Generally, methods of preparing iron oxide-silica supported reagents, iron oxide precursors were mixed with silica precursors in a solvent to form a "sol". Recently, Popovici and co-workers [51] produced iron oxide-silica supported reagents using a synthetic procedure that implements impregnating silica gels with anhydrous $\text{Fe}(\text{II})$ precursors followed by drying of the gels using ethanol. Maghemite dispersed nanoparticles doped in silica aerogels were yielded in a single-phase process. The nanocomposites showed a high saturation magnetization value and were superparamagnetic at ambient temperature. The success of his process is due to the impregnations of precursors after gelation, the exchange of water with ethanol before impregnation, and finally use of the anhydrous ferric salt.

Deng et al., reported that sol-gel method has also been used to synthesize magnetite and maghemite thin films, transparent iron-doped titanium oxide thin films, ferroelectromagnetic bismuth iron oxide films, mixed iron oxides, and iron oxide-alumina nanocomposites [52].

Disadvantages of the method of sol-gel approach, the contamination targeted product by byproducts of reactions, and the need for post-treatment of the products.

e) High pressure hydrothermal methods of preparation

These methods depend on the ability of water at elevated pressures and temperatures to hydrolyze and dehydrate metal salts, and the low solubility of the

produced metal oxides in water at these conditions to generate required super saturation [39]. The higher temperatures favor higher dehydration rates, and so does the high diffusivity of reactants in water at these conditions. High super saturations is achieved by this process because of the low solubility of metal hydroxides and oxides, to obtain the desired fine crystals. Variables such as pressure, temperature, reaction time, and the precursor product system can be adjusted for high nucleation rates and to control growth. The process is environmentally favored and versatile, since it does not demand organic solvents or post-treatments such as calcination. Consequently, high pressure hydrothermal processes have been widely investigated for the synthesis of metal oxides as powders, nanoparticles and single crystals [53].

Xu and Teja reported that the hydrothermal synthesis of iron oxides can also be performed in situ within porous structures. They also have successfully deposited hematite in the pores of activated carbon using supercritical water. The hematite nanoparticles were 16-36 nm in diameter and were uniformly distributed throughout the carbon pellets (see Fig. 2.13). The resulting activated carbon iron oxide nanoparticles were used as catalysts in the oxidation of propanal at rates that were an order of magnitude higher than those for activated carbon catalysts solely [54].

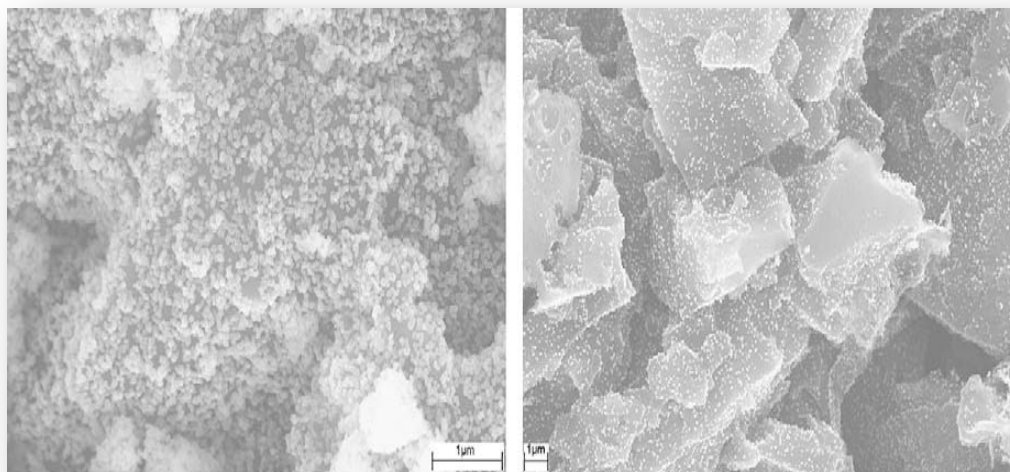


Fig. 2.13: Distribution of hematite nanoparticles deposited (a) on the surface and (b) in the interior of activated carbon pellets by supercritical water [54].

Darab and Matson [55] succeeded in using the hydrothermal method to synthesize fine iron oxide nanoparticles in a continuous flow reactor. Their method involves fast heating of flowing solutions by contact with supercritical water at residence times of 5 to 30s in the reactor to control growth. A schematic

roadmap of their experimental procedures is shown in Fig. 2.14. Hematite nanoparticles less than 10 nm in size were obtained from ferric nitrate and ferric ammonium sulfate solutions using this method. Magnetite nanoparticles were also synthesized using ferrous sulfate and urea reaction. It was observed that the particle size and

morphology were dependent on operating temperature and processing time. The particle size increased dramatically as the operating temperature increased and different forms of iron oxide were produced from the same precursor by elevating the temperature. For instance, mixtures of 6-line ferrihydrite and hematite were formed at 250-350°C, while pure hematite was obtained at temperatures higher than 350°C [55].

Adschiri and coworkers [56a] also introduced another flow technique, it used rapid and thorough mixing of the water stream with the precursor solution in a T-mixer. High super saturation rates were resulted in the T-mixer due to the low solubility of metalhydroxides in supercritical water. Hematite, magnetite, and other oxides were achieved in a size range of 1 nm to 10nm at temperature of 400-490°C and pressure of 30-40 MPa. The residence time of the precursor solutions was nearly 2 min in the experiments accomplished.

Cabanas and Poliakov, also studied the process of hydrolysis of metal acetates in supercritical water. They produced a number of oxides, including

magnetite, in the size range 3-105 nm at 200-400°C and 25 MPa [56b]. Teja and Koh also produced a Uniform particles of hematite using two variations of the continuous hydrothermal technique [57]. Hawa and co-workers [58], successfully synthesized 50 nm magnetite nanoparticles without the addition of a strong base using the continuous technique. The mixture of ferric ammonium sulfate, ferric nitrate, ferric sulfate, and ferrous chloride were used for the synthesis of hematite, while ferric ammonium citrate was used as a precursor for magnetite. In the magnetite experiments, Fe(III) reduced to Fe(II) by carbon monoxide. In this experiment CO was produced via the thermal decomposition of ammonium citrate. Since CO gas is miscible in supercritical water, it provided a uniform reducing atmosphere throughout the reaction. This implies that the product form can be managed by the control of an oxidizing or reducing gas during continuous hydrothermal process using above mentioned conditions.

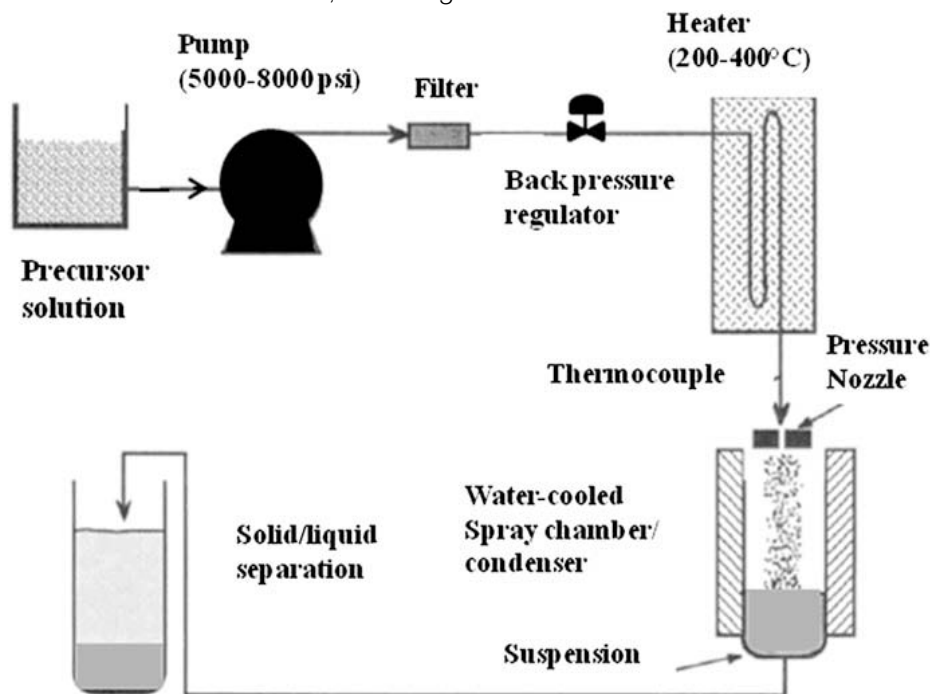


Fig. 2.14: Schematic diagram of the apparatus of Darab et al. 1998

Lester and his group [59] reported a design that takes advantage of differences in the densities of supercritical water and precursor solutions by using a nozzle mixer to improve mixing inside the reactor. The reactor diagram is shown in Fig. 2.15. The diagram shows supercritical water is introduced into the reactor from the top and the precursor metal salt stream from the bottom, upon mixing of the two streams allows for making use of buoyancy induced eddies to produce "ideal" mixing conditions. This leads to short residence times and limits subsequent particle growth. Lester and

his group synthesized a variety of metal oxides, for which size range from 6 to 64 nm, there by demonstrating the effectiveness of separation of nucleation and growth steps in continuous hydrothermal process. The continuous hydrothermal process offers various opportunities for controlling particle size and morphology, and this done by maintaining residence times low and mixing processes worthwhile. However, design of particle surfaces cannot be achieved in situ and requires additional post-processing steps.

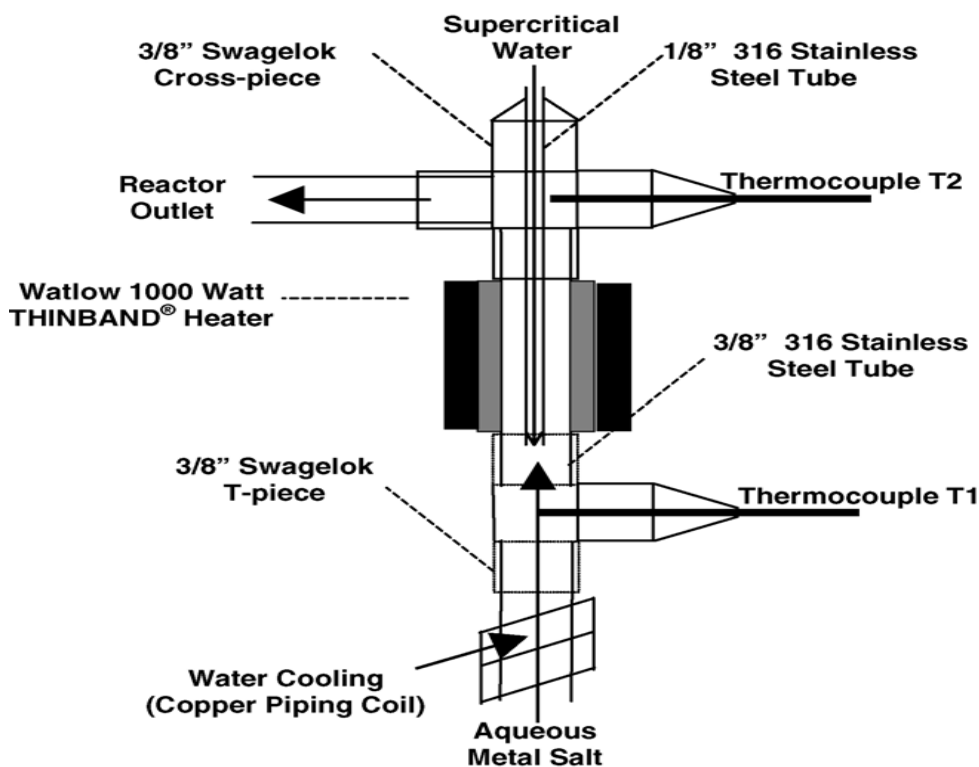


Fig. 2.15: Schematic of the nozzle mixer [59]

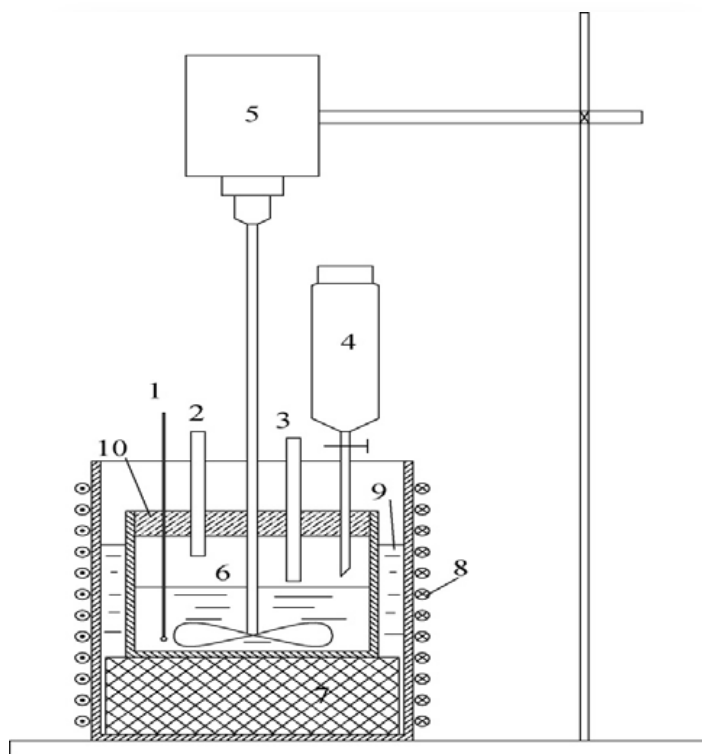
f) *Co-precipitation Method of preparation of metal oxide nanoparticles*

Co-precipitation method is a well-developed method and widely used in the preparations of nanoparticles metal oxides. The method takes advantage of the low solubility of an element in the soil solution than predicted by the solubility product, in addition to the solubility of an ion is lower in mixed ionic solution than in pure ionic solutions. The reason for the reduced solubility is due to co-precipitation. Co-precipitation process is as a result of incorporation of trace element into mineral structure during solid solution formation and recrystallization of minerals. This process will reduce the mobility of the trace elements that are incorporated into the mineral.

Minerals will only incorporate isomorphous elements into their structure through replacement of elements, these elements must have similar ionic radii for changing of the composition of the mineral. For example, during the formation of calcite, Mn^{2+} , Cd^{2+} , and Fe^{2+} can possibly be incorporated into the mineral structure. In the formation of Fe and Al-oxides, Cr^{3+} , Mn^{3+} , and V^{3+} may be incorporated into the structure. Mn and Fe-oxides have more possibility for co-precipitation than Al-oxides and aluminosilicate minerals such as clay and zeolites. Co-precipitation reactions are also controlled by the rate of soil mineral dissolution.

Wei and Viadero concluded that in order to achieve the precipitation of magnetite, the molar ratio of $[\text{Fe}_3] / [\text{Fe}_2]$ should be 2:1 at high pH [60]. Synthesis

system was used for this study at molar ratio of 1:2:8 for the Fe (II): Fe (III): OH and also de-oxygenated. This is to achieve phase purity of magnetite without the presence of impurities such as goethite and iron oxyhydroxide [61]. In this regard the green precipitate was observed when the Fe_2 ion initially added to the system followed by a brown precipitate was also resulted with the addition of Fe_3 ions in 1:2 ratio, as discussed earlier. When the alkaline NaOH was added into the mixed precursor of Fe_2 and Fe_3 ions, a thick black precipitate was observed and this was subsequently shown the resulting product is magnetite, as discussed by Schwertmann and Cornell [63].



Schematic diagram of synthesis system with solenoid . 1, Thermometer. 2, Condenser port. 3, N_2 gas. 4, Dropper. 5, Stirrer. 6, Reactor. 7 Cushion. 8, Electromagnetic solenoid. 9, Hot water bath. 10, Sealed rubber[62].

IV. CONCLUSION

This review article describes a substantial progress has been made in methods and applications of iron oxides nanoparticles, with emphasis on advances in nanotechnology and biotechnology. Several methods have been reported to show developments that implement control over physical properties, such as size, size distribution, shape, crystal structure, defect distribution and surface structure. Among the methods reviewed, Continuous Supercritical Co-precipitation method technique assures process control and scalability. Furthermore, this method is environmentally suitable, and the surface treatment of nanoparticles, however, requires additional steps. The method has been found to be very simple, easy to carry on, low cost, and higher yield and without the use of organic reagents.

The challenge for all methods is the design of magnetic nanoparticles with effective surface coatings that provide optimum performance in vitro and in vivo biological applications. Additional challenges include scale-up, toxicity, and safety of large-scale particle production processes. Numerous progress were made in the synthesis Fe_3O_4 Nanoparticles.

The aim in various industrial applications and technologies remain in the optimization of the processes leading to desirable nanoparticles, nevertheless technical complexity does not prevent access to

chemicals with high quality applications and specifications. The physical and chemical characteristics associated with these materials are often determined by the type and nature of the method used in the preparation. There is a disparity between the methods used depending on the economic cost and production capacity of each method. The differences in the use and application of prepared nanomaterials are also an important basis for different methods of preparation.

The increasing demand and advances for these materials since its inception has led to a wide range of methods for the production of high quality and quantitative materials, especially in the industrial fields (electronics and telecommunications), medical fields (different treatments and the manufacture of human alternatives). Or a huge economic cost. One of the most common features of all methods is to deal with the atomic scale (atom towards another atom) for the purpose of reaching a design that is considered in advance to obtain desired results. The difference in the scale of the mass of a single substance leads to different chemical effectiveness. The smaller the scale, the greater the chemical effectiveness due to the increased chemical impact of this substance.

On this basis, nanoscience and nanoscale preparation techniques are improving in accordance with the requirements of the global technological advances and expansion in various sectors. This allows

for great global competition to continue to arrive at the best results for better safe technology and quality of life.

REFERENCES RÉFÉRENCES REFERENCIAS

- Laís Salomão Arias, Juliano Pelim Pessan, Ana Paula Miranda Vieira, Taynara Maria Toito de Lima, Alberto Carlos Botazzo Delbem, and Douglas Roberto Monteiro, *Antibiotics (Basel)* 2018; v.7(2): 46.
- Riviere C., Roux S., Tillement O., Billotey C., Perriat P. Nano-systems for medical applications: Biological detection, drug delivery, diagnostic and therapy. *Ann. Chim. Sci. Mater.* 2006; 31: 351–367.
- Suri S.S., Fenniri H., Singh B. Nanotechnology-based drug delivery systems. *J. Occup. Med. Toxicol.* 2007; 2:16.
- Ochekpe N.A., Olorunfemi P.O., Ngwuluka N.C. Nanotechnology and drug delivery part 1: Background and applications. *Trop. J. Pharm. Res.* 2009; 8: 265–274.
- Niemirowicz K., Markiewicz K.H., Wilczewska A.Z., Car H. Magnetic nanoparticles as new diagnostic tools in medicine. *Adv. Med. Sci.* 2012; 57:196–207.
- Lazhen Shen, Bei Li, and Yongsheng Qiao, *Materials (Basel)*. 2018 ; 11(2): 324.
- Zhou Y., Chen M., Zhuo Y., Chai Y., Xu W., Yuan R. In situ electrodeposited synthesis of electrochemiluminescent Ag nanoclusters as signal probe for ultrasensitive detection of Cyclin-D1 from cancer cells. *Anal. Chem.* 2017; 89: 6787–6793.
- Han L., Zhang Y., Lu X., Wang K., Wang Z., Zhang H. Polydopamine nanoparticles modulating stimuli-responsive PNIPAM hydrogels with cell/tissue adhesiveness. *ACS Appl. Mater. Interfaces.* 2016; 8: 29088–29100.
- Kuang Y., Zhang K., Cao Y., Chen X., Wang K., Liu M., Pei R. Hydrophobic IR-780 dye encapsulated in cRGD-conjugated solid lipid nanoparticles for NIR imaging-guided photothermal therapy. *ACS Appl. Mater. Interfaces.* 2017; 9:12217–12226.
- Alam S.R., Shah A.S., Richards J., Lang N.N., Barnes G., Joshi N., MacGillivray T., McKillop G., Payne J., *Circ. Cardiovasc. Imaging.* 2012; 5: 559–565.
- Luong D., Sau S., Kesharwani P., Iyer A.K., *Biomacromolecules.* 2017; 18: 1197–1209.
- Nan X., Zhang X., Liu Y., Zhou M., Chen X., Zhang X., *ACS Appl. Mater. Interfaces.* 2017; 9:9986–9995.
- Paul Chen, Yanbin Li, Tianhong Cui, Roger Ruan, *international journal of agricultural and biological engineering*, Vol 6, No 1 (2013):122-155.
- Milad Fathi-Achachelouei, Helena Knopf-Marques, Cristiane Evelise Ribeiro da Silva, Julien Barthès, Erhan Bat, Aysen Tezcaner, and Nihal Engin Vrana, *Frontiers of bioengineering and biotechnology*, 2019,7(113):1-22.
- Edina C. Wang, and Andrew Z. Wang, *Integr Biol (Camb)*. 2014; 6(1): 9–26.
- Hill HD, and Mirkin CA., *Nat. Protocols.*, 2006: 324–336.
- Mashhadi Malekzadeh A., Ramazani A., Tabatabaei Rezaei S.J., and Niknejad H.. *J. Colloid Interface Sci.* 2017; 490:64–73.
- Monaco I., Arena F., Biffi S., Locatelli E., Bortot B., La Cava F., Marini G.M., Severini G.M., Terreno E., Comes Franchini M. *Bioconjugate Chem.* 2017; 28:1382–1390.
- Seeni R.Z., Yu X., Chang H., Chen P., Liu L., Xu C., *ACS Appl. Mater. Interfaces.* 2017; 9: 20340–2034
- Anselmo A.C., Mitragotri S. A review of clinical translation of inorganic nanoparticles. *AAPS J.* 2015; 17: 1041–1054.
- Clinicaltrials.gov. [(accessed on 7 May 2018)]; Available online: <https://www.clinicaltrials.gov/ct2/results?term=iron+oxide+nanoparticles>
- Laurent S., Forge D., Port M., Roch A., Robic C., Vander Elst L., Muller R. N. *Chem. Rev.* 2008; 108: 2064–2110.
- Vuong Q.L., Berret J., Fresnais J., Gossuin Y., Sandre O. *Adv. Healthc. Mater.* 2012; 1: 502–512.
- Niluka M. Dissanayake, Kelley M. Current, and Sherine O. Obare, *Int J Mol Sci.* 2015; 16(10): 23482–23516.
- Iglesias O., Labarta A. *Phys. Rev. B.* 2001; 63: 184416.
- Sun Y., Ma M., Zhang Y., Gu N. *Colloids Surf. Physicochem. Eng. Asp.* 2004; 245: 15–19.
- Amy S. Teja*, Pei-Yoong Koh, *Progress in Crystal Growth and Characterization of Materials*, 55 (2009): 22-45.
- Annye Pineau, Ndue Kanari, and I GABALLAH, *Thermochimica Acta* 456(2) 2007:75-88
- AG Roca, R Costo, AF Rebolledo, S Veintemillas-Verdaguer, P Tartaj, T Gonzalez-Carreno, MP Morales, CJ Serna, *Journal of Physics D: Applied Physics*, 42(22), 2009:22-40.
- M. Mahmoudi, A. Simchi, and M. Imani, *Journal of the Iranian Chemical Society* 7, 2010:S1–S27.
- Edina C. Wang and Andrew Z. Wang, *Integr Biol (Camb)*. 2014; 6(1): 9–26.
- Hyon Bin Na, In Chan Song, and Taeghwan Hyeon, *advanced Materials*, V.21(21), 2009 : 2133-2148.
- Cai W, Gao T, Hong H, and Sun J, *Journals of Nanotechnology, Science and Applications*, v. 1, 2008: 17–32.
- Bautista F M, Campelo J M, Luna D, Marinas J M, Quiros R A and Romero A, *Appl. Catal.* 2007. B70 611.
- Hongping HE, Yuanhong ZHONG, Xiaoliang LIANG, Wei TAN, Jianxi ZHU, and Christina Yan WANG, *Scientific Reports*, 5, 2015, 10139.
- Javad Tavakoli. *J Mech Behav Biomed Mater.* 2017; 65: 373-382.

37. Thomas Ming Swi Chang, *Artificial Cells, Nanomedicine, and Biotechnology*, 47(1) 2019: 997-1013.
38. Sungho Park, Sangho Lim, and Choi H. *ChemInform*, 18(22), 2006:112-133.
39. Singh M.P., Shalini, K., Shivashankar S. A., Deepak G. C., Bhat, N. & Shripathi, T., *Materials Chemistry and Physics* 110, 2008: 337-343.
40. A. Tavakoli, M. Sohrabi, A. Kargari, *Chemical Papers* 61 (3) (2007) 151-170.
41. R. Alexandrescu, V. Bello, V. Bouzas, R. Costo, F. Dumitrache, M. A. García, R. Giorgi, M. P. Morales, I. Morjan, C. J. Serna, and S. Veintemillas-Verdaguer, *AIP Conference Proceedings* 1275, 22 (2010); 11-34.
42. C. Jäger, H. Mutschke, F. Huisken, R. Alexandrescu, I. Morjan, F. Dumitrache, R. Barjega, I. Soare, B. David, and O. Schneeweiss, *Applied Physics A*, v.85, 2006 pages53–62.
43. Oscar Bomati-Miguel, Lena Ma zeina, Alexandra Navrotsky, and Sabino Veintemillas-Verdaguer, *Chem. Mater.*, 20, 2, 2008: 591–598.
44. Charles, S W, Rovensweig. *J. Magn. Magn. Mat.* 39, 1983: 190–22
45. S. Khalafalla, and G. Reimers, *IEEE Transactions on Magnetics*, v 16(2), 1980: 178 – 183.
46. Josef Kopp, Petr Novak, Josef Kaslik, and Jiri Pechousek, *Acta Chim. Slov.*, 66, 2019: 455–465.
47. Sun, C., Jerry, S., Lee, H. & Zhang, M., *Advanced Drug Delivery Reviews* 60, 2008: 1252–1265.
48. Pedro Tartaj, Mar'ia del Puerto Morales, Sabino Veintemillas-Verdaguer, Teresita Gonz'alez-Carreno and, Carlos J Serna, *J. Phys. D: Appl. Phys.* 36 (2003) R182–R197.
49. Ignác Capek, *Polymer Journal* v. 26, 1994:1154–1162.
50. V. Pillai, P. Kumar, M. J. Hou, P. Ayyub, D.O. Shah, *Advances in Colloid and Interface Science* 55 (1995):241-269.
51. Gupta A. K. & Gupta, M., *Biomaterials* 26(18), 2004: 3995-4021.
52. L. Casas, A. Roig, E. Molins, J.M. Grenèche, J. Asenjo, and J. Tejada, *Applied Physics Av.* 74, 2002: 591–597.
53. M. Popovici, and Cecilia Savii, *Journal of Optoelectronics and Advanced Materials* 7(5), 2005: 234-250.
54. Deng Y. H., Wang C. C., Hu J. H., Yang W. L. & Fu S. K. *Colloids and Surfaces A: Physicochemical and Engineering Aspects* 262, 2005: 87-93.
55. Hiromichi Hayashi, and Yukiya Hakuta, *Materials*, 3, 2010: 3794-3817.
56. Xu, C., and Teja, A. S., *The Journal of Supercritical Fluids* 44, 2008: 85-91.
57. Darab, J. & Matson, D., *Journal of Electronic Materials* 27(10) 1998:1068-1072.
58. Tadafumi Adschiri, Yukiya Hakuta, and Kunio Arai, *Ind. Eng. Chem. Res.* 2000, 39, 12, 4901–4907
59. Cabanas, A. & Poliak off. M., *Journal of Materials Chemistry* 11(5) 2001:1408-1416.
60. Teja A.S, and Koh P.Y., *Progress in Crystal Growth and Characterization of Material*, s 55, 2009: 22-45
61. Hawa C.Y., Mohamed, F., Chia C.H., Radiman, S., Zakaria, S., Huang N.M., and Lim H.N.
62. *Ceramics International*, 1 36, 2010: 1417–1422.
63. Lester, E., Blood, P., Denyer, J., Giddings, D., Azzopardi, B., and Poliak off, M., *The Journal of Supercritical Fluids* 37, 2006: 209-214.
64. Xinchao Wei, and Roger C. Viadero Jr, *Colloids and Surfaces A: Physicochemical and Engineering Aspects*, 294 (1–3), 2007: 280-286.
65. Gnanaprakash, G., Mahadevan, S., Jayakumar, T., Kalyanasundaram, P., Philip, J. & Baldev Raj., *Materials Chemistry and Physics*, 103, 2007: 168-175.
66. Hua, D, and Wang, Y., *Particuology* 7, 2009: 363–367.
67. U. Schwertmann, and R. M. Cornell, *Iron Oxides in the Laboratory: Preparation and Characterization* 1991: 5-18.